Nanostructures

International Edition: DOI: 10.1002/anie.201506874
German Edition: DOI: 10.1002/ange.201506874

From Atomistic Surface Chemistry to Nanocrystals of Functional Chalcogenides

*Volker L. Deringer and Richard Dronskowski**

chalcogenides · density functional calculations · materials science · nanostructures · surfaces

Synthesis and utilization of nanocrystals are highly active fields of current research, but they require a thorough understanding of the underlying crystal surfaces. In this Minireview, we span the arc from surfaces to free nanocrystals, and onward to their chemical synthesis, using as examples lead selenide (PbSe), tin telluride (SnTe), and their direct chemical relatives. Besides experimental insights, we highlight the increasingly influential role played by quantum-chemical simulations of surfaces and nanocrystals. What can theory do today, or possibly tomorrow; where are its limits? Answering these questions, and skillfully linking them to experiments, could open up new atomistically (that is, chemically) guided perspectives for nanosynthesis.

1. Introduction

The synthesis of atomically well-defined structures has always been a central target of chemistry. The ongoing exploration of the nanoscale has not changed this—on the contrary, it gives rise to new functionalities, aesthetic geometric structures at times, as well as a healthy dose of interdisciplinarity.[1] Today, rationally planned syntheses afford nanocrystals with precise size and shape control,[2] and beyond these isolated building blocks, researchers aim to construct so-called "superlattices":[3] freshly synthesized nanocrystals are precisely assembled to form, as "pseudo-atoms", well-ordered packing schemes, such as cubic body-centered or cubic close-packed.[3a]

Not only in this case does the relationship to traditional solid-state chemistry become apparent: many ingredients of nanochemistry have been listed in Gmelin's classical handbook for decades, and this holds in particular for the chalcogenides of the fourth main group ("IV–VI semiconductors").[4] The lead salts PbS and PbSe today are found in solar cells[5] or photodetectors,[6] whereas PbTe is used in nanostructured thermoelectrics;[7] finally, SnTe established the materials class of topological crystalline insulators[8] which have fascinating electronic properties: conducting at the surface, insulating in the bulk. Understandably, these compounds have evolved into prototypes of nanoscale materials, in chemistry and beyond.

In addition to creative synthetic and analytic techniques, the toolkit of nanochemistry is increasingly augmented by quantum-chemical simulations which are mostly carried out using density-functional theory (DFT). Today, theory is no longer restricted to "only" reproducing experimental data, but can often unfold predictive power of its own: recent successful examples include tailor-made magnetic intermetallics,[11] transparent conducting materials,[12] or biocompatible alloys.[13] We do believe that realistic simulations and, ultimately, quantum-chemically supported synthesis planning could likewise be targets for nanochemistry; long-term targets, but highly desirable ones.

In this Minireview, we aim to push this quest forward. We face the task in a "retrosynthetic" way, that is to say: we must move from superlattices back to single nanocrystals, and understand shape and properties of the single nanocrystals based on the individual surfaces involved (Figure 1). Thereby, we implicitly assume thermodynamic control: the more stable a particular surface, the more it contributes to the crystal shape. Hence, kinetic aspects are, for the time being, ignored in this approximation,[14] and we will discuss cases where doing so is justified; nonetheless, we stress that nucleation and growth of nanocrystals can be simulated nowadays, as well.[15]

[*] Dr. V. L. Deringer, Prof. Dr. R. Dronskowski
Institute of Inorganic Chemistry
RWTH Aachen University
Landoltweg 1, 52056 Aachen (Germany)
E-mail: drons@HAL9000.ac.rwth-aachen.de
Prof. Dr. R. Dronskowski
Jülich-Aachen Research Alliance (JARA-HPC)
RWTH Aachen University
52056 Aachen (Germany)

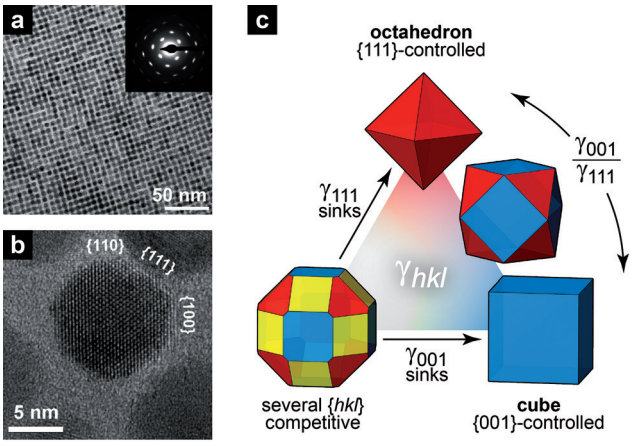

Figure 1. Lead selenide (PbSe) in nanocrystalline form and the link to the underlying crystal facets. a) Well-ordered 2D superstructure, recorded using transmission electron microscopy (TEM); the electron-diffraction pattern (inset) shows the single-crystallinity.[3b] Adapted with permission from Ref. [3b]. Copyright 2013 American Chemical Society. b) TEM close-up of a single nanocrystal; the facets involved are labeled.[9] Reprinted with permission from Ref. [9]. Copyright 2010 American Chemical Society. c) Basic crystal morphologies in the rocksalt type, determined by the ratio of surface energies γ_{hkl}. Visualization was done using VESTA.[10]

Table 1 provides an overview and thus also an outline for the following Sections. For reasons of brevity, we focus on the IV–VI semiconductors. For the backgrounds of the theoretical methods, we refer the reader to excellent texts on ab initio surface chemistry[16] and the modeling of nanoparticles.[17]

2. Free Surfaces

Manufacturing isolated, free surfaces is achieved by epitaxy—traditionally a specialty of semiconductor physics, but also of electrical engineering—and has a long and proud history in the field of IV–VI compounds.[20] Besides electrical measurements, the structures at surfaces have been of prime interest from the beginning. For example, the ideal rocksalt-type (111) surfaces are densely covered exclusively by one atomic species: that is, in lead selenide, completely covered by Pb or completely covered by Se—or a reconstruction is formed (in crystal-chemical language: a 2D superstructure) to saturate the bonds that had previously been cut apart. To clarify this structural question, Rutherford backscattering was applied to PbSe(111) and later to PbTe(111):[21] both showed Pb-terminated reconstructions and thus no dense surfaces. Likewise, the near-surface bond lengths were explored early on, for example, by low-energy electron diffraction (LEED) on PbTe(001).[22] We stress that both methods, notwithstanding their clear advantages, do not allow for direct observations of the surfaces, and thus detective work is often needed to characterize the atomic structures.

Theory, if carefully used, can be a useful tool to complement experiment. For surface modeling, DFT with periodic basis sets has been well established: to do so, a suitably oriented slab is theoretically cleaved from the crystal structure and surrounded with artificial vacuum (Figure 2).

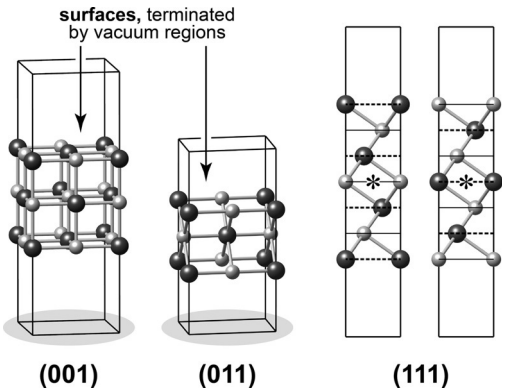

Figure 2. Schematic drawing of slab models for the most important crystal surfaces in the rocksalt type, deliberately disregarding reconstructions for now. Both the slabs and the vacuum regions are significantly larger in computational practice; in particular, simulations of (111) reconstructions require laterally expanded supercells. On the right-hand side, the inversion centers have been marked by asterisks.

This technique was applied to lead chalcogenide (001) surfaces early on, initially with regard to structural parameters and with the above-mentioned experiments setting the bar.[23] Besides structures, however, the simulation also yields

Volker Deringer (born 1987 in Ingolstadt, Germany) studied chemistry at RWTH Aachen University, received his diploma in 2010 and his doctorate in 2014 under guidance of Richard Dronskowski. He worked on the quantum-chemical modeling and bonding analysis of complex solids, in particular regarding their surfaces. In October 2015, he started postdoctoral research at the University of Cambridge as a fellow of the Alexander von Humboldt Foundation.

Richard Dronskowski (born 1961 in Brilon, Germany) studied chemistry and physics in Münster and obtained his doctorate under guidance of Arndt Simon (Stuttgart) in 1990. After a stay as a visiting scientist with Roald Hoffmann (Cornell) he received his habilitation in Dortmund and, in 1996, moved to RWTH Aachen University where he holds the Chair of Solid-State and Quantum Chemistry. His research fields comprise experimental solid-state chemistry (carbodiimides, guanidinates, nitrides, metastable phases), neutron diffraction, and the quantum chemistry of solids (electronic structure, bonding theory, magnetism, thermochemistry).

Table 1: Experimental methods for exploring surfaces and nanocrystals, and complementary quantum-chemical approaches (necessarily greatly simplified).

Object	Property	Experiment	Theory
Isolated surfaces	Atomic structure and stability	Diffraction and scattering (e.g., LEED)	**DFT slab models** (Section 2)
	Surface band structure	Angle-resolved photoelectron spectroscopy (ARPES)	DFT and tight-binding band-structure computations[18]
Free nanocrystals	Morphology	Transmission electron microscopy (TEM)	**Wulff construction** (Section 3)
	Electronic properties	Spectroscopy	DFT energy levels of entire nanocrystals[19]
Ligand–nanocrystal interactions	Surface species and their bonding	Spectroscopy	**DFT slab models** (Section 4)
	Composition and morphology	Quantification (AAS, MS), imaging (TEM)	DFT and multiscale simulations of ligand-covered particles[17]

total energies (which usually steer the structural optimization); this makes the surface energy γ immediately accessible, unlike in experiments. The previously shown (001) and (011) models contain both atom types in equal amounts; their γ are then obtained by comparing the computed energy of the supercell ("SC") to that of the crystalline AB phase [Eq (1)]:

$$\gamma = \frac{1}{2A}\left[E_{SC} - N_{AB} \times E_{AB}^{(cryst)}\right] \quad (1)$$

Thereby, the supercell contains N_A formula units and, at both sides, exposes surfaces of area A. If the surfaces are not stoichiometric ($N_A \neq N_B$), an additional term enters the equation which depends on the chemical potential μ_i, that is, on the components' availability, say, of element A [Eq. (2)]:[24]

$$\gamma = \frac{1}{2A}\left[E_{SC} - N_{AB} \times E_{AB}^{(cryst)} - (N_A - N_B)\mu_A\right] \quad (2)$$

This approach allows access to the dense rocksalt-type (111) surfaces, as well (Figure 2, right).[25] Generally, γ is thus a function of the chemical-potential landscape; its plot for various competing surfaces is called the "surface phase diagram".[24] In Figure 3a, as an example, we show one for PbTe:[26] in harmony with chemical intuition, the charge-neutral (001) surface is lowest and γ_{001} is constant ($N_{Pb} = N_{Te}$), whereas the energies of both dense (111) alternatives come out significantly higher. Among the (111) surfaces, the Te-terminated one—denoted $(111)_{Te}$—is more favorable over a wide range, because at least formally it corresponds to a fully filled electron octet; $(111)_{Pb}$, on the other hand, exhibits "dangling bonds" and is less favorable. The availability of lead, expressed via μ_{Pb}, grows from left to right, and the energy of the $(111)_{Pb}$ surface is lowered concomitantly. Nonetheless, neither of the two dense, polar surfaces is stable with regard to reconstructions (Figure 3b), as investigated in detail in Ref. [26]. Vertical lines demarcate the accessible range of potentials, which stems from thermodynamic laws and can be quantified using DFT.[24]

What do such diagrams mean in practice? As Hoffmann remarked in a highly readable Essay, computations (also for nanochemical questions) are seldom about pure numbers, at least primarily, but instead aim to recognize, understand, and utilize chemical trends.[28] An instructive example was con-

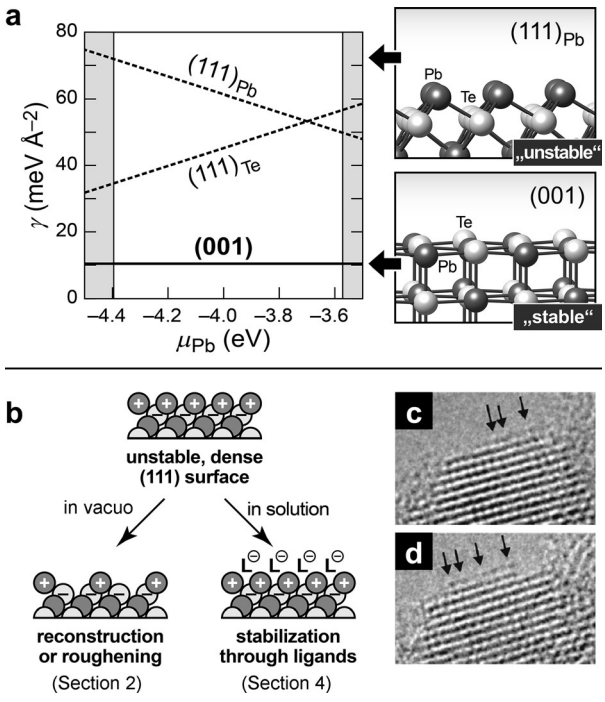

Figure 3. a) Surface phase diagram for selected, dense PbTe surfaces. Adapted with permission from Ref. [26]. Copyright 2013 American Chemical Society. b) Simplified scheme for stabilizing dense surfaces: in vacuum, they either form well-defined reconstructions (in the example shown, every second surface cation is missing) or exhibit surface "roughening".[27] In solution, suitable ligands may stabilize the surfaces (Section 4). c,d) "Nanofaceting" as a special case of surface roughening at PbSe(111), as observed in TEM images. Reprinted with permission from Ref. [9]. Copyright 2010 American Chemical Society.

tributed by Fang et al. who first computed surface energies of PbSe; as in Figure 3a, the dense (111) surfaces emerged as being unstable.[9] Experiments then showed that {111} facets of PbSe nanocrystals are indeed unstable after ligand removal and quickly crumble on the atomic scale (Figure 3c,d). Such formation of "rough" surfaces is known, for example, from metal oxides, where roughening likewise eliminates unstable surfaces (and gives rise to interesting reactivities),[27] in addition to the above-mentioned precise reconstructions. That being said, the globally most-stable option for the lead chalcogenides is given by the charge-neutral (001) surface (Figure 3a), and in nice agreement with this prediction, annealing ultimately leads to {001}-dominated PbSe nanostructures.[9]

3. From Crystal Facets to Nanocrystals

Knowing about the isolated surfaces—and having computed their stabilities—entire nanocrystals can now be studied. A truly classical approach is based on the Gibbs–Wulff theorem,[29] according to which a crystal attempts to minimize the sum of surface energies involved. Once the surface energies have been computed from first principles, a polyhedron which predicts the equilibrium morphology of a particle can be seamlessly constructed. Today, this technique is widely used in materials chemistry and physics.[30]

We have recently been interested in the nanomorphology of SnTe.[31] The compound, despite homologous composition, strongly stands out from the heavier lead salts: while neither PbSe nor PbTe expose unreconstructed (111) faces,[9,26] dense tellurium-covered SnTe(111) surfaces are either stable or they are not, depending on the chemical environment. Likewise, the predicted Wulff polyhedron varies from strongly truncated to cuboctahedral to an almost perfect cube (Figure 4a).

The experimental confirmation followed in the same year and was likewise supported by DFT computations.[32] In particular, Li et al. succeeded in linking a rather abstract quantity (μ_{Te}) to a measurable one, namely, the tellurium partial pressure, and thus to the real synthetic conditions.[32] In the laboratory, tuning thus becomes available: at low temperatures, a vapor–liquid–solid (VLS) route[33] leads to {111}-dominated nanostructures; at higher temperature, the volatile tellurium evaporates, which lowers μ_{Te} and raises γ_{111}, and almost perfectly cubic nanocrystals are formed (Figure 4). The theoretical prediction is thus smoothly confirmed—entirely due to the thermodynamic control. Subsequent syntheses by other groups confirmed these findings,[34] and experimental aspects of shape-controlled SnTe nanostructures have recently been summarized in an interesting article.[35]

Wulff constructions are primarily done in vacuum, but conceptionally they are by no means restricted to the vacuum. It is possible to translate interface energies into a Wulff construction for embedded crystallites, as Leitsmann et al. have shown for PbTe nanocrystals in a CdTe matrix.[36] These computations were validated by high-resolution TEM experiments.[36b] Even more complex models have been proposed which incorporate additional parameters and afforded impressive results, among others, for TiO_2[37] or CdS[38] nanocrystals. A similar "charting" of nanoscale IV–VI semiconductors could now indeed be valuable, and not only for academic interest.[39]

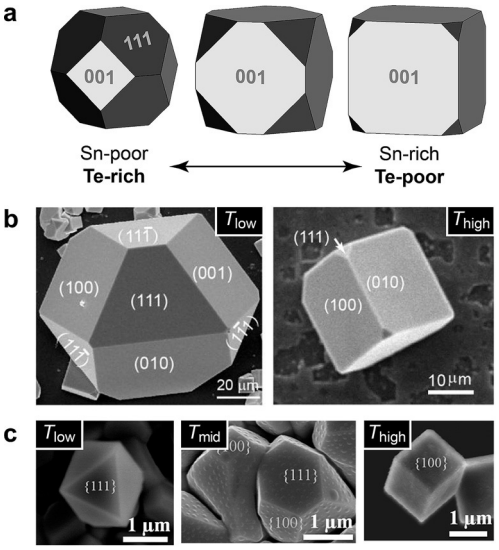

Figure 4. a) Wulff polyhedra for SnTe, based on DFT-computed surface energies.[31] Copyright 2013 Wiley-VCH, Weinheim. b) Experimental verification at the hand of SnTe crystallites grown at different temperatures. Adapted with permission from Ref. [32]. Copyright 2013 American Chemical Society. c) Likewise, from another study. Adapted with permission from Ref. [34b]. Copyright 2014 American Chemical Society.

Let us not forget to point out the limits of the theories described above, and thereby to answer one of the questions posed in the Abstract. Necessarily founded on thermodynamics, the present approach cannot capture kinetic barriers, but these barriers can be game-changing especially when studying wet-chemical syntheses. DFT models are usually rather small, owing to the limited computational power, and simply cannot reflect too complex structures.[40] And: there are cases where atomic structure and nanomorphology do not "fit" at all,[41] and then the theory presented herein does not stand any chance.

4. Ligands and Wet-Chemical Synthesis

Whereas the previous Section was concerned with free nanocrystals grown by vapor-phase deposition, there is a second pathway: wet-chemical syntheses proceed via suitable, mainly organic ligands[42] which can directly influence reactions and product properties.[28,43] In this Section, we highlight atomistic insight into ligand-covered surfaces and chemically synthesized nanocrystals,[44] again from a combined perspective of experiment and theory.

As regards theory, Argeri et al.[45] studied the behavior of typical ligands on PbSe surfaces: trioctylphosphine oxide (TOPO), hexylamine, oleic acid, and oleate. "Chopping off" the hydrocarbon units enabled DFT simulations (Figure 5a): naturally, propionic acid differs from oleic acid (right-hand side of Figure 5a) in physical properties, but the chemical

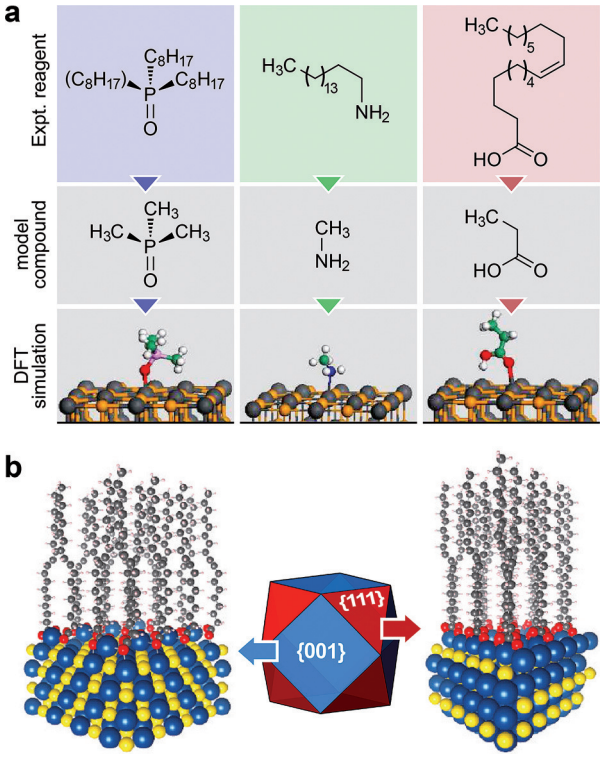

Figure 5. a) Typical ligands used in the synthesis of PbSe nanocrystals and the way toward their quantum-chemical modeling.[45] Structural drawings adapted with permission from Ref. [45]. Copyright 2011 American Chemical Society. b) DFT modeling of oleate ligands on the different crystal surfaces of PbSe. Adapted with permission from Ref. [46]. Copyright 2012 American Chemical Society.

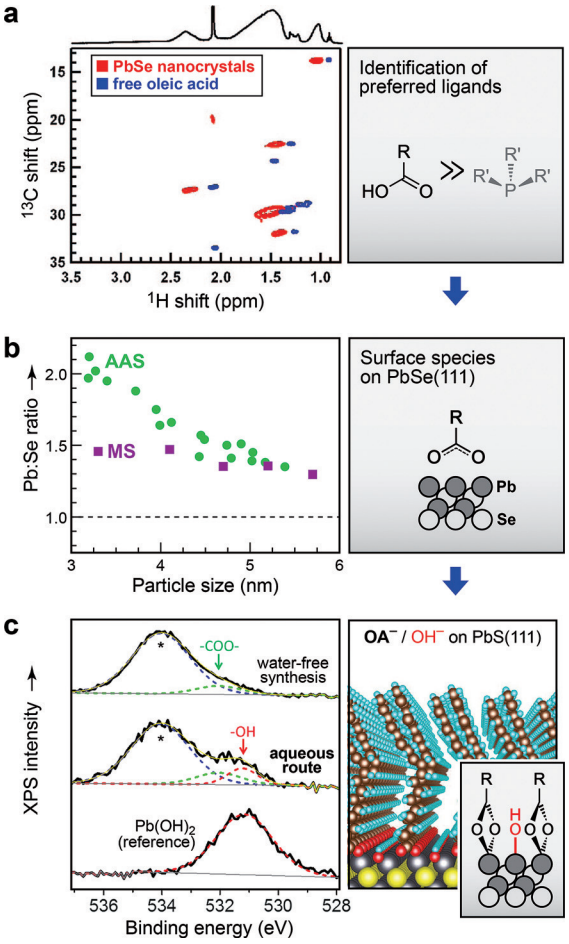

Figure 6. Experimental and theoretical insight into the surfaces of wet-chemically synthesized nanocrystals. a) 2D NMR spectra, overlaid for free oleic acid (blue) and PbSe nanocrystals (red). Adapted with permission from Ref. [47]. Copyright 2008 American Chemical Society. b) Experimental Pb:Se ratios for differently sized PbSe particles, determined in independent studies by mass spectrometry (data from Ref. [48]; ■) and by atomic absorption spectroscopy (data from Ref. [49]; ●). c) XPS data for PbS nanocrystals obtained by two different synthesis routes (left), and atomistic models explaining the hydroxylation observed (right). From Ref. [50]. Adapted with permission from AAAS.

bonding of the acid group directly at the surface will be similar, and only this bonding is of interest for the moment. It is necessary to emphasize the fundamental importance of careful chemical modeling which is required because of chronically sparse computing power—a curse or a blessing, depending on perspective, but in any case an ever-recurring theme in the interplay of theory and experiment.

Later, Bealing et al.[46] succeeded in simulating entire ligands (Figure 5b) and, much more importantly, in extending and generalizing the PbSe Wulff shape (Section 3) to adsorbate-covered surfaces. In this way, new and more general relationships for nanomorphology can be delineated, which now additionally becomes dependent on the surface coverage and is particularly influenced by contrasts in adsorption behavior. For example, according to Lewis' acid–base concept, it seems chemically intuitive that a carboxylate ligand ($RCOO^-$) is more attracted by a cation-covered (111) surface than by its neutral (001) counterpart.[45,46] These predictions were verified by directed syntheses at variable ligand concentrations and using TEM experiments.[46]

Experimentalists have additional local probes at their disposal. In a seminal work, Moreels et al. clarified the identity of preferred ligands and how they interact with the nanoscopic substrate.[47] For synthesis, lead acetate is initially treated with oleic acid, whereas elemental selenium is mixed with TOP; finally, both solutions are combined,[42,48] which makes two types of ligands principally possible. After isolating the as-synthesized PbSe nanocrystals, however, only oleic acid shows its "fingerprint" in the two-dimensional NMR spectrum (Figure 6a).

The composition of nanocrystals can also yield important insight, indirectly so. The rocksalt-type (001) surfaces are stoichiometrically precise (Section 2), and so are {001}-controlled particles, whereas octahedral, {111}-dominated ones need not be. Experimentally, it was now possible to measure this very Pb:Se ratio of nanocrystals: by mass spectrometry,[48] and by atomic absorption spectroscopy[49] (Figure 6b). Apparently, oleate-covered PbSe nanocrystals prefer octahedral shapes, and thus Pb-terminated (111) surfaces, as sketched on the right-hand side of Figure 6b; this Pb excess can also be rationalized at the hand of theoretical shape factors.[45] Upon heating (and "burning away" the ligands), cubes are obtained instead, because

among the naked surfaces (001) is more favorable after all (Section 2).

Recently published work has elucidated the properties of PbS(111) surfaces as a function of reaction partners.[50] Figure 6c shows XPS spectra for two different synthetic routes, water-free or in aqueous solution. Only in solution is the presence of hydroxide ions detected. Theoretical modeling provides an atomistic picture: OH^- ions squeeze in between the bulky oleate ligands.

From what has been said so far, the conceptual way finally leads onward to oxidation processes. Again, we consider adsorbates on chalcogenide surfaces, but oxidation is usually an unwanted effect. The microscopic processes have been studied, for example, on GeTe(111), using experiments (XPS)[51] and DFT slab models.[52] Earlier work instructively showed how near-surface sulfide ions on PbS(001) get oxidized all the way to sulfate species.[53] For tin chalcogenide nanocrystals in particular, ^{119}Sn Mössbauer spectroscopy turned out to be a useful local probe.[54] Finally, a joint experimental–theoretical study showed how oxidation processes can not only be understood, but ultimately prevented: PbSe(001) surfaces were covered with halide ions and thus protected them from decay.[55]

5. Summary and Outlook

In this Minireview, we have shown a way of going from isolated surfaces to nanocrystals, using new bridges built between experiment and theory. Deliberately, we have focused on lead salts and on SnTe, but we want to give at least a brief outlook along chemical relationships: to the aforementioned cadmium chalcogenides,[38,44] but also upward to metal oxides, whose nanocrystals likewise fascinate by virtue of new synthetic routes and properties.[56] The rocksalt type, naturally, is only found in some of these cases, and more complex structures likewise call for the use of more complex slab models.

The huge materials class of oxides also serves to illustrate methodological challenges. At times, transition-metal oxides create massive problems for DFT computations,[57] and even for PbTe (which is more good-natured in this regard) the absolute surface energies depend on the choice of DFT functional.[26] Fortunately, new developments are in progress, such as the random phase approximation[58] or multireference methods for extended systems.[59] The routine use of such highly expensive techniques for surfaces and adsorbates is still in the future, but should be a worthwhile goal; the skillful creation of models will be mandatory once more, as it has been for the first DFT computations (Section 4).

Ultimately, however, better computational methods will not change the basic concepts: the tools are at hand today, at least in principle, and in the future, jointly obtained atomistic understanding must support the planning of new syntheses. This could concern the choice of materials, but also that of ligands, maybe even their rational design? Theory and experimental probes, judiciously used together, could furthermore give valuable guidance for the "bottom-up" assembly of nanocrystal superlattices.

Acknowledgements

We thank Philipp Konze and Dr. Adam Slabon for helpful discussions and suggestions. Our work on chalcogenide surfaces has been supported by the Deutsche Forschungsgemeinschaft (SFB 917 "Nanoswitches") and the Studienstiftung des deutschen Volkes (Ph.D. scholarship for V.L.D.) and furthermore profited from JARA-HPC computer time.

How to cite: *Angew. Chem. Int. Ed.* **2015**, *54*, 15334–15340
Angew. Chem. **2015**, *127*, 15550–15557

[1] Among the wealth of interesting Highlight and Review articles, we mention but one: M. V. Kovalenko, L. Manna, A. Cabot, Z. Hens, D. V. Talapin, C. R. Kagan, V. I. Klimov, A. L. Rogach, P. Reiss, D. J. Milliron, P. Guyot-Sionnnest, G. Konstantatos, W. J. Parak, T. Hyeon, B. A. Korgel, C. B. Murray, W. Heiss, *ACS Nano* **2015**, *9*, 1012–1057.

[2] Y.-w. Jun, J.-s. Choi, J. Cheon, *Angew. Chem. Int. Ed.* **2006**, *45*, 3414–3439; *Angew. Chem.* **2006**, *118*, 3492–3517.

[3] a) J. J. Choi, C. R. Bealing, K. Bian, K. J. Hughes, W. Zhang, D.-M. Smilgies, R. G. Hennig, J. R. Engstrom, T. Hanrath, *J. Am. Chem. Soc.* **2011**, *133*, 3131–3138; b) W. H. Evers, B. Goris, S. Bals, M. Casavola, J. de Graaf, R. van Roij, M. Dijkstra, D. Vanmaekelbergh, *Nano Lett.* **2013**, *13*, 2317–2323; c) M. P. Boneschanscher, W. H. Evers, J. J. Geuchies, T. Altantzis, B. Goris, F. T. Rabouw, S. A. P. van Rossum, H. S. J. van der Zant, L. D. A. Siebbeles, G. Van Tendeloo, I. Swart, J. Hilhorst, A. V. Petukhov, S. Bals, D. Vanmaekelbergh, *Science* **2014**, *344*, 1377–1380.

[4] a) D. V. Talapin, J.-S. Lee, M. V. Kovalenko, E. V. Shevchenko, *Chem. Rev.* **2010**, *110*, 389–458; b) M.-R. Gao, Y.-F. Xu, J. Jiang, S.-H. Yu, *Chem. Soc. Rev.* **2013**, *42*, 2986–3017; c) V. L. Deringer, R. Dronskowski, M. Wuttig, *Adv. Funct. Mater.* **2015**, 25, 6343–6359; d) V. L. Deringer, Dissertation, RWTH Aachen, **2014**.

[5] A. J. Nozik, M. C. Beard, J. M. Luther, M. Law, R. J. Ellingson, J. C. Johnson, *Chem. Rev.* **2010**, *110*, 6873–6890.

[6] G. Konstantatos, E. H. Sargent, *Nat. Nanotechnol.* **2010**, *5*, 391–400.

[7] G. J. Snyder, E. S. Toberer, *Nat. Mater.* **2008**, *7*, 105–114.

[8] a) T. H. Hsieh, H. Lin, J. Liu, W. Duan, A. Bansil, L. Fu, *Nat. Commun.* **2012**, *3*, 982; b) Y. Tanaka, Z. Ren, T. Sato, K. Nakayama, S. Souma, T. Takahashi, K. Segawa, Y. Ando, *Nat. Phys.* **2012**, *8*, 800–803.

[9] C. Fang, M. A. van Huis, D. Vanmaekelbergh, H. W. Zandbergen, *ACS Nano* **2010**, *4*, 211–218.

[10] K. Momma, F. Izumi, *J. Appl. Crystallogr.* **2011**, *44*, 1272–1276.

[11] a) R. Dronskowski, K. Korczak, H. Lueken, W. Jung, *Angew. Chem. Int. Ed.* **2002**, *41*, 2528–2532; *Angew. Chem.* **2002**, *114*, 2638–2642; b) B. P. T. Fokwa, H. Lueken, R. Dronskowski, *Chem. Eur. J.* **2007**, *13*, 6040–6046.

[12] F. Yan, X. Zhang, Y. G. Yu, L. Yu, A. Nagaraja, T. O. Mason, A. Zunger, *Nat. Commun.* **2015**, *6*, 7308.

[13] D. Raabe, B. Sander, M. Friák, D. Ma, J. Neugebauer, *Acta Mater.* **2007**, *55*, 4475–4487.

[14] Separating thermodynamic from kinetic control is as important on the nanoscale as it is for all of chemistry. Recent introductions are found in a) Y. Wang, J. He, C. Liu, W. H. Chong, H. Chen, *Angew. Chem. Int. Ed.* **2015**, *54*, 2022–2051; *Angew. Chem.* **2015**, *127*, 2046–2079; b) Y. Xia, X. Xia, H.-C. Peng, *J. Am. Chem. Soc.* **2015**, *137*, 7947–7966.

[15] J. Anwar, D. Zahn, *Angew. Chem. Int. Ed.* **2011**, *50*, 1996–2013; *Angew. Chem.* **2011**, *123*, 2042–2061.

[16] A. Groß, *Theoretical Surface Science: A Microscopic Perspective*, Springer, Berlin, **2009**.

[17] A. S. Barnard, *Rep. Prog. Phys.* **2010**, *73*, 086502.
[18] For an instructive example of the application of experiment and theory to SnTe see P. B. Littlewood, B. Mihaila, R. K. Schulze, D. J. Safarik, J. E. Gubernatis, A. Bostwick, E. Rotenberg, C. P. Opeil, T. Durakiewicz, J. L. Smith, J. C. Lashley, *Phys. Rev. Lett.* **2010**, *105*, 086404.
[19] For example (SnTe, PbSe, PbTe): R. Leitsmann, F. Bechstedt, *ACS Nano* **2009**, *3*, 3505 – 3512.
[20] Extensive work on thin films of the compounds discussed herein may be found, for example, in J. N. Zemel, J. D. Jensen, R. B. Schoolar, *Phys. Rev.* **1965**, *140*, A330 – A342.
[21] a) PbSe: K. Kimura, K. Nakajima, Y. Fujii, M. Mannami, *Surf. Sci.* **1994**, *318*, 363 – 367; b) PbTe: T. Nakajima, K. Kimura, M. Mannami, *Nucl. Instrum. Methods Phys. Res. Sect. B* **1998**, *135*, 350 – 354.
[22] A. A. Lazarides, C. B. Duke, A. Paton, A. Kahn, *Phys. Rev. B* **1995**, *52*, 14895 – 14905.
[23] a) A. Satta, S. de Gironcoli, *Phys. Rev. B* **2000**, *63*, 033302; b) J. X. Ma, Y. Jia, Y. L. Song, E. J. Liang, L. K. Wu, F. Wang, X. C. Wang, X. Hu, *Surf. Sci.* **2004**, *551*, 91 – 98.
[24] a) Seminal work on the ab initio thermochemistry of surfaces goes back to K. Reuter, M. Scheffler, *Phys. Rev. B* **2001**, *65*, 035406; b) a nice overview is given in a DFT study on structurally (albeit not chemically) related MnO(111) surfaces: C. Franchini, V. Bayer, R. Podloucky, G. Parteder, S. Surnev, F. P. Netzer, *Phys. Rev. B* **2006**, *73*, 155402.
[25] A special case is given by GeTe, which is rhombohedrally distorted; by a small modification in slab construction, the (111) surfaces can be modeled nonetheless: V. L. Deringer, M. Lumeij, R. Dronskowski, *J. Phys. Chem. C* **2012**, *116*, 15801 – 15811.
[26] V. L. Deringer, R. Dronskowski, *J. Phys. Chem. C* **2013**, *117*, 24455 – 24461.
[27] T. E. Madey, W. Chen, H. Wang, P. Kaghazchi, T. Jacob, *Chem. Soc. Rev.* **2008**, *37*, 2310 – 2327, and references therein.
[28] R. Hoffmann, *Angew. Chem. Int. Ed.* **2013**, *52*, 93 – 103; *Angew. Chem.* **2013**, *125*, 99 – 111.
[29] G. Wulff, *Z. Kristallogr. Mineral.* **1901**, *34*, 449 – 530.
[30] a) N. Moll, A. Kley, E. Pehlke, M. Scheffler, *Phys. Rev. B* **1996**, *54*, 8844 – 8855; b) L. Wang, F. Zhou, Y. S. Meng, G. Ceder, *Phys. Rev. B* **2007**, *76*, 165435; c) T. Lee, B. Delley, C. Stampfl, A. Soon, *Nanoscale* **2012**, *4*, 5183 – 5188.
[31] V. L. Deringer, R. Dronskowski, *ChemPhysChem* **2013**, *14*, 3108 – 3111.
[32] Z. Li, S. Shao, N. Li, K. McCall, J. Wang, S. X. Zhang, *Nano Lett.* **2013**, *13*, 5443 – 5448.
[33] The VLS method, introduced half a century ago, is a key procedure for making nanowires: a) R. S. Wagner, W. C. Ellis, *Appl. Phys. Lett.* **1964**, *4*, 89 – 91; b) A. M. Morales, C. M. Lieber, *Science* **1998**, *279*, 208 – 211; c) Y. Wu, P. Yang, *J. Am. Chem. Soc.* **2001**, *123*, 3165 – 3166.
[34] a) M. Saghir, M. R. Lees, S. J. York, G. Balakrishnan, *Cryst. Growth Des.* **2014**, *14*, 2009 – 2013; b) M. Safdar, Q. Wang, M. Mirza, Z. Wang, J. He, *Cryst. Growth Des.* **2014**, *14*, 2502 – 2509; c) J. Shen, Y. Jung, A. S. Disa, F. J. Walker, C. H. Ahn, J. J. Cha, *Nano Lett.* **2014**, *14*, 4183 – 4188.
[35] J. Shen, J. J. Cha, *Nanoscale* **2014**, *6*, 14133 – 14140.
[36] a) R. Leitsmann, L. E. Ramos, F. Bechstedt, *Phys. Rev. B* **2006**, *74*, 085309; b) R. Leitsmann, L. E. Ramos, F. Bechstedt, H. Groiss, F. Schäffler, W. Heiss, K. Koike, H. Harada, M. Yano, *New J. Phys.* **2006**, *8*, 317.
[37] A. S. Barnard, L. A. Curtiss, *Nano Lett.* **2005**, *5*, 1261 – 1266.
[38] A. S. Barnard, H. Xu, *J. Phys. Chem. C* **2007**, *111*, 18112 – 18117.
[39] The "treasure hunt" for functional materials according to suitable coordinates is underway, as well: D. Lencer, M. Salinga, B. Grabowski, T. Hickel, J. Neugebauer, M. Wuttig, *Nat. Mater.* **2008**, *7*, 972 – 977.
[40] T. Milek, D. Zahn, *CrystEngComm* **2015**, *17*, 6890 – 6894.
[41] In a recently reported case, the morphology suggests a highly symmetric crystal structure, whereas the particle is amorphous inside: T. Saltzmann, M. Bornhöfft, J. Mayer, U. Simon, *Angew. Chem. Int. Ed.* **2015**, *54*, 6632 – 6636; *Angew. Chem.* **2015**, *127*, 6732 – 6736.
[42] A key contribution to wet-chemical synthesis, on which many later studies are based, is found in C. B. Murray, S. H. Sun, W. Gaschler, H. Doyle, T. A. Betley, C. R. Kagan, *IBM J. Res. Dev.* **2001**, *45*, 47 – 56.
[43] Besides the widely used organic ligands described herein, other species can also be thought of, say, molecular chalcogenides: M. V. Kovalenko, M. Scheele, D. V. Talapin, *Science* **2009**, *324*, 1417 – 1420.
[44] While we focus on IV – VI semiconductors once more, such atomistic approaches are of paramount interest for other compounds as well. For an excursion to molecular insights into cadmium chalcogenide nanocrystals see, for example, J. Vela, *J. Phys. Chem. Lett.* **2013**, *4*, 653 – 668.
[45] M. Argeri, A. Fraccarollo, F. Grassi, L. Marchese, M. Cossi, *J. Phys. Chem. C* **2011**, *115*, 11382 – 11389.
[46] C. R. Bealing, W. J. Baumgardner, J. J. Choi, T. Hanrath, R. G. Hennig, *ACS Nano* **2012**, *6*, 2118 – 2127.
[47] I. Moreels, B. Fritzinger, J. C. Martins, Z. Hens, *J. Am. Chem. Soc.* **2008**, *130*, 15081 – 15086.
[48] I. Moreels, K. Lambert, D. De Muynck, F. Vanhaecke, D. Poelman, J. C. Martins, G. Allan, Z. Hens, *Chem. Mater.* **2007**, *19*, 6101 – 6106.
[49] Q. Dai, Y. Wang, X. Li, Y. Zhang, D. J. Pellegrino, M. Zhao, B. Zou, J. Seo, Y. Wang, W. W. Yu, *ACS Nano* **2009**, *3*, 1518 – 1524.
[50] D. Zherebetskyy, M. Scheele, Y. Zhang, N. Bronstein, C. Thompson, D. Britt, M. Salmeron, P. Alivisatos, L.-W. Wang, *Science* **2014**, *344*, 1380 – 1384.
[51] L. V. Yashina, R. Püttner, V. S. Neudachina, T. S. Zyubina, V. I. Shtanov, M. V. Poygin, *J. Appl. Phys.* **2008**, *103*, 094909.
[52] V. L. Deringer, R. Dronskowski, *J. Appl. Phys.* **2014**, *116*, 173703.
[53] L. V. Yashina, A. S. Zyubin, R. Püttner, T. S. Zyubina, V. S. Neudachina, P. Stojanov, J. Riley, S. N. Dedyulin, M. M. Brzhezinskaya, V. I. Shtanov, *Surf. Sci.* **2011**, *605*, 473 – 482.
[54] A. de Kergommeaux, J. Faure-Vincent, A. Pron, R. de Bettignies, B. Malaman, P. Reiss, *J. Am. Chem. Soc.* **2012**, *134*, 11659 – 11666.
[55] J. Y. Woo, J.-H. Ko, J. H. Song, K. Kim, H. Choi, Y.-H. Kim, D. C. Lee, S. Jeong, *J. Am. Chem. Soc.* **2014**, *136*, 8883 – 8886.
[56] For example: H. Dong, Y.-C. Chen, C. Feldmann, *Green Chem.* **2015**, *17*, 4107 – 4132.
[57] V. I. Anisimov, J. Zaanen, O. K. Andersen, *Phys. Rev. B* **1991**, *44*, 943 – 954.
[58] L. Schimka, J. Harl, A. Stroppa, A. Grüneis, M. Marsman, F. Mittendorfer, G. Kresse, *Nat. Mater.* **2010**, *9*, 741 – 744.
[59] a) G. H. Booth, A. Grüneis, G. Kresse, A. Alavi, *Nature* **2013**, *493*, 365 – 370; b) E. Voloshina, B. Paulus, *J. Chem. Theory Comput.* **2014**, *10*, 1698 – 1706.

Received: July 24, 2015
Revised: September 3, 2015
Published online: November 13, 2015

